Carbohydrate Polymers 94 (2013) 807–813

Contents lists available at SciVerse ScienceDirect

Carbohydrate Polymers

journal homepage: www.elsevier.com/locate/carbpol

Efficient enzymatic hydrolysis of the bagasse pulp prepared with active oxygen and MgO-based solid alkali

Tujun Xie [a,*], Lu Lin [b,*], Chunsheng Pang [a], Junping Zhuang [a], Jianbin Shi [a], Qiulin Yang [a]

[a] State Key Laboratory of Pulp and Paper Engineering, South China University of Technology, Guangzhou 510640, Guangdong, China
[b] School of Energy Research, Xiamen University, Xiamen 361005, Fujian, China

ARTICLE INFO

Article history:
Received 3 July 2012
Received in revised form 15 January 2013
Accepted 23 January 2013
Available online 13 February 2013

Keywords:
Bagasse
Solid-base pulp
Enzymatic hydrolysis

ABSTRACT

The enzymatic hydrolysis of the bagasse pulp prepared from the treatment process with active oxygen and MgO-based solid alkali was studied. The hydrolysates were tested by IC (ionic chromatography) for the analysis of monosaccharide. Additionally, the changes of pulp before and after hydrolysis were characterized with Fourier transform infrared spectroscopy (FTIR), scanning electron microscopy (SEM), X-ray diffraction (XRD), Kajaani cellulose automatic analyzer and atomic force microscopy (AFM) techniques. The results showed that an optimized sugar yield of 82.38% was obtained at the substrate concentration of 5% for 72 h with the enzyme dosage of 15 IU/g. Furthermore, as the length of the cellulose fiber decreased, the crystallinity of cellulose increased, and more depressions appeared on the surface of pulp after enzymatic hydrolysis.

1. Introduction

With gradual depletion of petroleum and other fossil resources, abundant renewable lignocellulose material is regarded as the most important industrial raw material in the future (Caputo, Palumbo, Pelagagge, & Scacchia, 2005; Rogers & Brammer (2009); Uihlein, Ehrenberger, & Schebek, 2008; Yoshioka, Hirata, Matsumura, & Sakanishi, 2005). Lignocellulose biomass has long been recognized as a potential sustainable source of mixed sugars for fermentation to biofuels and biomaterials. Bagasse, as one of the abundant plant cellulose resources, has been partly used for producing useful chemicals such as monosaccharide and organic acids, but the practical scale is small, and the techniques are mostly traditional methods such as strong acid hydrolysis.

Lignocellulose is a natural macromolecule and forms a complex crystalline structure that is resistant to enzymatic attack and insoluble in water (Schacht, Zetzl, & Brunner, 2008). Therefore, the lignocellulose must be pretreated before enzymatic hydrolysis in order to change the structure of cellulose and remove lignin (Ardersen, 1998; Elisabet, Marcus, & Anders, 2005; Wei, Kim, & Flemmin, 2003).

Currently, the pretreatment techniques prior to enzymatic hydrolysis include physical methods (steam explosion, radiation, freezing, etc.) and chemical methods (acid, alkali, organic solvent, etc.) (Sun & Cheng, 2002). To date, several researchers have reported some pretreatment techniques for bagasse. For instance, He, Rallming, Weidong, and Shuangfei (2010) investigated the effect of enzymatic hydrolysis by pretreating bagasse with mixed solutions of hydrogen peroxide and acetic acid and obtained lignin removal up to 97.09%. Carrascoa et al. (2010) described a treatment process with steam and the catalyst of SO_2 to study the effect of enzymatic hydrolysis of bagasse and a sugar yield of 87% was obtained.

In present processes of biomass utilization, pretreatment is a key step. Cellulose and some hemi-cellulose are separated from the lignocellulose through the removal of lignin, and then are hydrolyzed and transformed. However, there exist some problems of high energy consumption, low efficiency and serious pollution in the traditional pretreatment techniques, respectively. Therefore, this study tries to investigate the hydrolysis characteristics of bagasse pulp prepared from the treatment process with active oxygen and MgO-based solid alkali. Presently, limited attention has been paid to this pretreatment technique. For instance, Chunsheng et al. (2012) had researched the changes of the surface structure of corn stalk in the cooking process with active oxygen and MgO-based solid alkali. The results showed that the lignin was effectively removed by active oxygen cooking with solid base, and the surface characteristic of single fiber changed to be granular. Xie, Lin, Pang, Yang, and Shi (2011) investigated the enzymatic hydrolysis of bagasse pulp prepared from the different treatment process with active oxygen and MgO-based solid alkali and obtained the following optimum pretreatment conditions: temperature (165 °C), initial oxygen pressure (1.0 MPa), dosage of H_2O_2 (1.5 wt%, based on the oven dried weight of corn stalk), dosage of solid alkali (15.0 wt%, based on the oven dried weight of bagasse), liquor-to-stalk ratio (6:1, w/w) and pretreatment time (2 h). The sugar yield following

* Corresponding authors. Tel.: +86 0592 5952786.
E-mail addresses: xietujun2006@163.com (T. Xie), lclulin@scut.edu.cn (L. Lin).

0144-8617/$ – see front matter © 2013 Elsevier Ltd. All rights reserved.
http://dx.doi.org/10.1016/j.carbpol.2013.01.071

enzymatic hydrolysis was 52.36% for these pretreatment conditions.

Furthermore, the treatment process with Mg-based solid alkali and active oxygen is considered as a clean method without emission of noxious gases and liquids and the insoluble solid base could be recycled. The active oxygen comes from O_2 and H_2O_2, and the solid base is MgO. The purpose of this paper is mainly to investigate the conditions of enzymatic hydrolysis of solid base pulp of bagasse, to discover the changes to cellulose before and after enzymatic hydrolysis, in order to provide another method for the utilization of bagasse biomass.

2. Materials and methods

2.1. Materials

Bagasse was kindly supplied by Fengyun Co. Ltd. in China. Oxygen (purity of 99%) was bought from an industrial gas company, and hydrogen peroxide (30 wt%; Hongyan Reagent Factory of Tianjin, China) was diluted to the appropriate concentration when it was needed. The solid alkali used in this study was magnesium oxide powder (purity ≥98.0%, CAS No. 1309-48-4), which was obtained from Tianjin Kermel Chemical Reagents Co. Ltd., China. Cellulase, from *Trichoderma reesei* ATCC 26921, which the activity was 75 FPU/mL. Cellobiase (*Novozyme 188*) from *Aspergillus niger*, its activity was 500 IU/mL.

2.2. Pretreatment method

Bagasse was cooked at a liquor-to-stalk ratio of 6.0 (w/w), with an insoluble solid alkali content of 15.0 wt% (based on the oven dried (o.d.) weight of bagasse). Additionally, a 1.5 wt% dosage of hydrogen peroxide and an initial oxygen pressure of 1.0 MPa were used. Cooking was performed at 165 °C for 2 h, with a heating rate of 1 °C/min. The cooking was performed in a 2 L stainless, rotating autoclave, using 50 g of bagasse (o.d.).

2.3. Enzymatic hydrolysis

The bagasse pulp was hydrolyzed by a mixture of enzymes (cellulase and cellobiase). According to the properties of cellulase and cellobiase, the temperature and pH of enzymatic hydrolysis was fixed at 50 °C and 5.0, respectively for all experiments. To explore the optimized dose of enzyme, the experiment was performed at a substrate concentration of 5% for 72 h and adding enzymes at each enzyme dose of 5, 10, 15, 20, 30, 40 and 60 IU/g dry bagasse pulp, respectively. Besides, the amount of enzyme of 15 IU/g dry bagasse pulp and substrate concentration of 5% was fixed to explore the effect of different enzyme treatment times. The times used were 6, 12, 24, 48, 72 and 96 h. Moreover, the experiment to obtain the optimized substrate concentration was performed at the amount of enzyme of 15 IU/g dry bagasse pulp for 72 h and the substrate concentration was set up at 3%, 5%, 8%, 10% and 15%.

2.4. Sugar testing

The hydrolysates were tested by IC (ionic chromatography) for analysis of monosaccharide. The yield of sugar was calculated using the following formulae:

$$Y_g = \frac{L_g}{L_h} \times 100\% \quad (1)$$

$$Y_x = \frac{L_x}{L_h} \times 100\% \quad (2)$$

$$Y_s = \frac{L_x + L_g}{L_h} \times 100\% \quad (3)$$

where the Y_g, Y_x and Y_s are the yield of glucose, xylose and total sugar, the L_g, L_x and L_h are the quantity of glucose in the hydrolysates, the quantity of xylose in the hydrolysates and the quantity of holocellulose of the bagasse pulp, respectively.

2.5. Fourier transform infrared spectroscopy (FTIR)

The bagasse pulp before and after hydrolysis were tested by FTIR (Bruker Tensor 27, Germany). The samples were dried before testing. FTIR spectra were obtained on an FT-IR spectrophotometer (Bruker) using a KBr disc containing 1% finely ground samples. Thirty-two scans were taken of each sample recorded from 4000 to 400 cm^{-1} at a resolution of 4 cm^{-1} in the transmission mode.

2.6. Scanning electron microscopy (SEM)

The samples were washed with deionized water and dried using a vacuum drying oven for 72 h before testing. The dried samples were then coated with Au and visualized using a scanning electron microscope (S-3700N; Hitachi, Japan) at 10 kV.

2.7. X-ray diffraction (XRD)

X-ray diffraction (XRD) patterns of the samples were carried out using a BRUKER D8 Advance X-ray diffractometer with Cu Ka radiation source operated at 40 kV and 40 mA. Data was collected from 2θ between 5° and 60° with a step of 0.02° at a scanning speed of 3°/min.

2.8. Kajaani cellulose automatic analyzer

The cellulose before and after hydrolysis was analyzed by Kajaani cellulose automatic analyzer (FS-300).

2.9. Atomic force microscopy (AFM)

The AFM images were recorded with a Nanoscope IIIa microscope (Digital Instruments, Veeco Metrology Group) and a MFP-3D (Asylum Research, USA) in taping mode. The dried samples were fixed to a mica sheet and tested by AFM.

3. Results and discussion

3.1. The sugar yield for different conditions of enzymatic hydrolysis

The effect of sugar yield on different conditions of enzymatic hydrolysis was investigated, and the experiments were carried out at different enzyme treatment times, different amounts of enzyme and different substrate concentrations. It can be observed from Fig. 1 that the sugar yield increased along with the higher of the amount of enzyme and the longer enzyme treatment time, but reduced with higher of substrate concentrations.

It can be noted from Fig. 1a that the glucose yield and sugar yield increased from 43.05% and 2.12% to 52.80% and 29.58% when increasing the enzyme loading from 5 IU/g to 15 IU/g. However, when the enzyme loading was up to 15 IU/g, the total sugar yield was about 85.00%. This finding suggests that the amount of enzyme (more than 15 IU/g) is excessive.

As also can be seen from Fig. 1b, the process of enzymatic hydrolysis included 3 parts: initial stage (0–24 h), medium term (24–72 h) and the later stage (72–96 h). In the initial stage, the sugar yield improved quickly, the total sugar yield of 24 h (55.58%) was 1.8

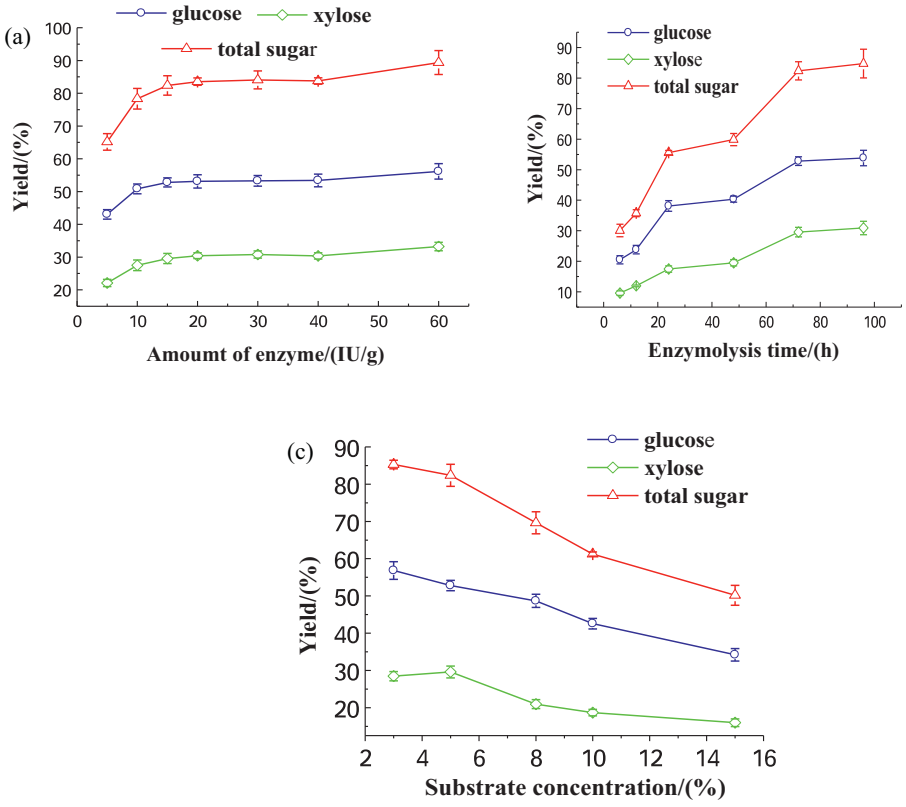

Fig. 1. The sugar yield for different conditions of enzymatic hydrolysis.

times as much as the 6 h (30.08%). This finding showed the concentration of effective enzyme was higher and the concentration of hydrolysates was lower in the initial stage resulted in faster hydrolysis rate to promote sugar yield. In the medium term, the total sugar yield also elevated along with the longer of enzymolysis time (from 55.58% to 82.38%), but the sugar yield improved more slowly. This is due to some hydrolysates that can inhibit the enzyme activity accumulate to reduce the hydrolysis reaction. In the later stage, the sugar yield had almost no change. It resulted from the accumulation of hazardous matter. The hazardous matter inhibited the enzyme activity, resulted in reducing the rate of enzymatic hydrolysis. In addition, this was related to the lower concentration of substrate.

Additionally, Fig. 1c shows that the total sugar yield changed more slowly (from 85.28% to 69.63%) when increasing the concentration of substrate from 3% to 8%. While the concentration of substrate was from 8% to 15%, the sugar yield changed more quickly, and the total sugar yield of 8% (69.63%) was 1.38 times as much as the 15% (50.17%). The concentration of substrate has a significant effect on the sugar yield. An explanation on the role of the substrate concentration is that lower concentration could accelerate mass transfer and the adsorption of enzyme. In addition, there are less inhibitory effects at lower substrate concentrations. Therefore, considering enzymatic efficiency and economy, the optimal conditions for enzymatic hydrolysis of bagasse pulp were chosen to be as follows: the amount of enzyme (15 IU/g), treatment time (72 h) and the concentration of substrate (5%).

3.2. Fourier transform infrared spectroscopy (FTIR)

The surface of chemical group changes was determined by FTIR. The FTIR spectra are shown in Fig. 2 and indicated three main areas of change in the spectra. According previous work (Stark & Matuana, 2007), the band at a wavenumber of 3400 cm^{-1} is the absorption peaks of hydroxyl of the intramolecular hydrogen bond of cellulose. In the process of enzymatic hydrolysis, the intensity of this peak decreased. This finding showed that the intramolecular hydrogen bond of cellulose and the crystalline structure of cellulose had been disrupted. Therefore, the cellulase can penetrate the interface between the cellulose molecules resulting in the degradation of cellulose. The band at the wavenumber of 1637 cm^{-1} corresponds to the absorption peaks of adsorbed water. During the process of enzymatic hydrolysis, the intensity of this peak firstly increased then decreased. This change indicated that the adsorbed water had changed. In the initial stage of enzymatic hydrolysis, the

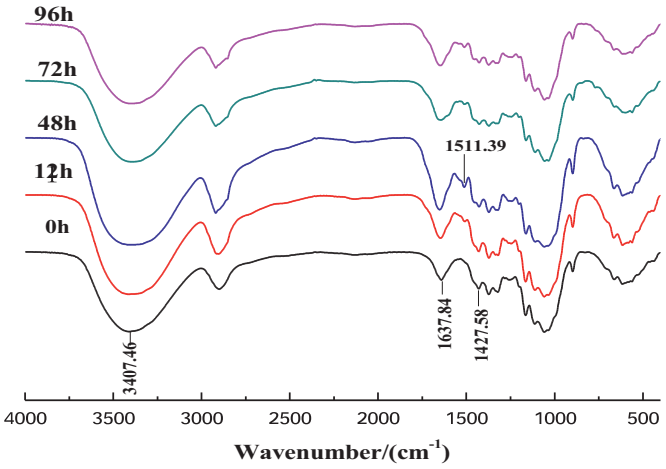

Fig. 2. The FTIR spectra of bagasse solid base pulp after enzyme hydrolysis for different times. (For interpretation of the references to color in this figure legend, the reader is referred to the web version of this article.)

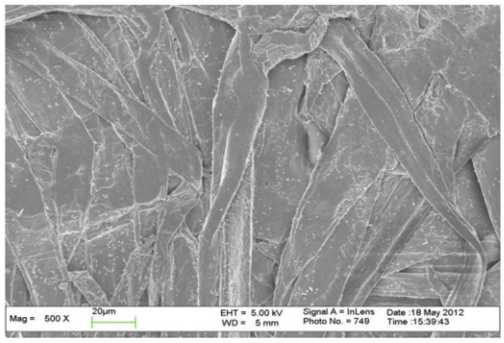

（a）oh (500×)

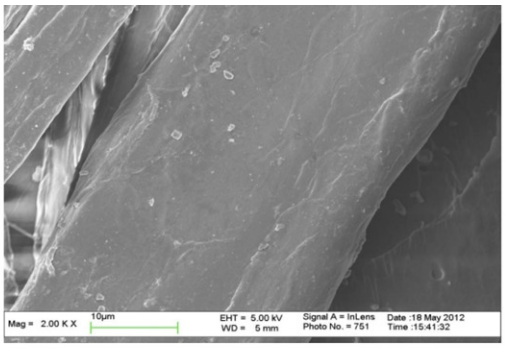

（b）0h (2000×)

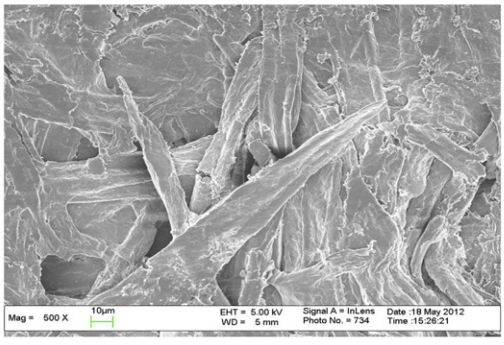

(c) 12h (500×)

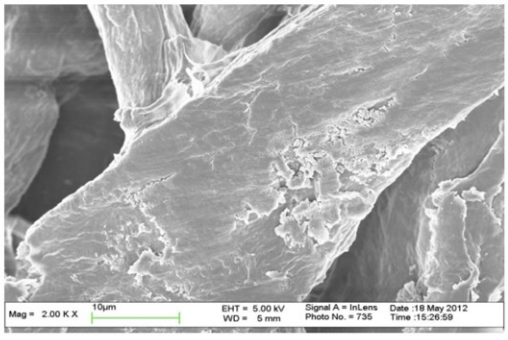

(d) 12h (2000×)

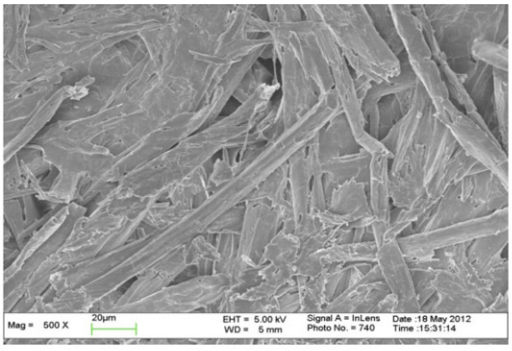

(e) 48h (500×)

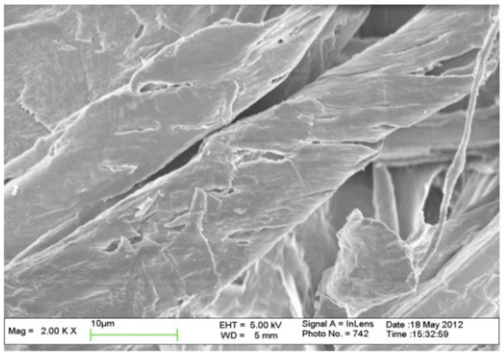

(f) 48h (2000×)

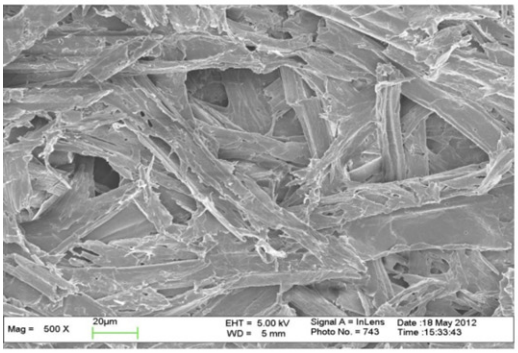

(g) 72h (500×)

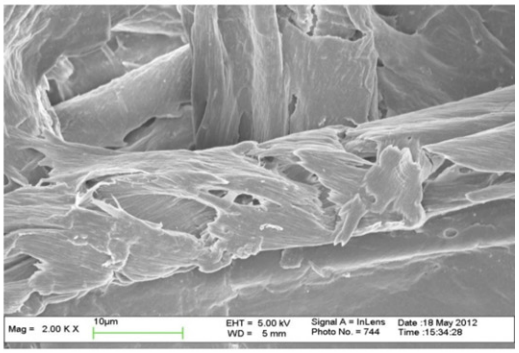

(h) 72h (2000×)

Fig. 3. The SEM pictures of bagasse solid base pulp after enzyme hydrolysis for different times.

cellulose absorbed water as a result of expansion so that the intensity of this peak enhanced. However, the enzyme infiltrated into the fiber and replaced some adsorbed water with the longer enzymatic treatment time resulted in the downgrading of this peak. The band at the wavenumber of 1511 cm^{-1} is the absorption peaks of benzene. The intensity of this peak increased with the enzymatic hydrolysis. An explanation of this phenomenon is that the cellulose degraded so that the content of lignin increased during the process of enzymatic hydrolysis. The absorption peak appeared at 1427 cm^{-1}, which showed the mixed structure of crystalline and non-crystalline regions appeared at the cellulose of pulp (Nelson & O'connor, 1964) and the proportion of the crystalline region was slightly higher.

3.3. Scanning electron microscopy (SEM)

Fig. 3 shows the SEM pictures of bagasse pulp after enzyme treatment for different times. Before enzymatic hydrolysis, the fiber of bagasse pulp was relatively complete. However, some small wrinkles, regarded as fine fibers, appeared on the surface of fiber (Fig. 3a and b). In the initial stage (Fig. 3c and d), the phenomenon of peeling layers by layers appeared on the surface of fiber and the surface of fiber was coarse. Moreover, there existed small holes on the surface of fiber. This finding showed that the enzyme attack the surface of fiber at first. In the medium term (Fig. 3e and f), some small trenches appeared on the surface of fiber and the holes increased. In addition, the small pieces on the surface of fiber reduced. This finding showed that the small pieces of fiber were mainly hydrolyzed in this stage. In the later stage (Fig. 3g and h), the fibers were not complete and became small pieces. However, the phenomenon of skin peeling was clearly observed on the surface of fiber.

3.4. X-ray diffraction (XRD)

Fig. 4 shows the XRD patterns of bagasse pulp after enzyme treatment for different times. The XRD pattern had three typical peaks of cellulose, at the 2θ of 15.7° (1 0 1), 21.5° (0 0 2), and 34.5° (0 0 4), respectively. Fig. 4 indicates that the position (1 0 1, 0 0 2, 0 4 0) of crystal face diffraction peak of cellulose had not changed, and the crystal face diffraction peak position of 0 0 2 appeared at 21.50° before and after enzymatic hydrolysis. This indicated that the crystalline region of bagasse pulp did not have a significant change after enzymatic hydrolysis, that the distance of the cellulose crystal layer did not changed. However, the intensity of the crystal surface (0 0 2) increased at first and then decreased during the process of enzymatic hydrolysis.

Table 1
The crystallinity of pulp following enzyme hydrolysis for different times.

Sample	0 h	12 h	48 h	72 h	96 h
I_{002}, Cps	4778	10,702	5284	4318	4085
I_{am}, Cps	2628	2803	1835	1452	1559
Crystallinity, %	45.00	73.81	65.27	66.37	61.84

The following formula is used for the calculation of the crystallinity index (Cao & Tan, 2005):

$$\text{Crystallinity} = \frac{I_{002} - I_{am}}{I_{002}} \times 100\%; \quad (4)$$

where I_{002} is peak intensity corresponding to 0 0 2 lattice plane of cellulose molecule, which is observed at 2θ equal to 22.5°, and I_{am} (at 2θ = 19°) is the peak intensity corresponding to cellulose. The crystallinities of bagasse pulp after enzyme treatment for different times are shown in Table 1. It can be noted from Table 1 that the crystallinity of cellulose firstly increased then decreased with the enzymatic hydrolysis. In the initial stage (0–12 h) of enzymatic hydrolysis, the degree of crystallinity of cellulose increased (from 45.00% to 73.81%). One reason may be that the enzymes mostly attack the amorphous region of cellulose resulted in increasing the size of crystalline. In the medium term (12–48 h) of enzymatic hydrolysis, the enzyme mainly attacked the crystalline region of cellulose resulted in decreasing the crystallinity of cellulose (from 73.81% to 65.27%). In the later stage (72–96 h) of enzymatic hydrolysis, the crystallinity of cellulose changed a little. Perhaps this was because the cellulase mainly penetrated the internal region of fiber in this stage resulting in little change in the crystalline regions of cellulose.

3.5. The length analysis of cellulose

Fig. 5 shows fiber length-weighted distribution of cellulose. It can be noted from Fig. 5 that the L_w became shorter after enzymatic hydrolysis, and was mainly between 0.1 mm and 0.5 mm. This result indicated that the cellulose of bagasse pulp was mainly hydrolyzed into small fibers after enzymatic hydrolysis.

As also can be seen from Table 2, the length and coarseness of cellulose became smaller, and the amount of fines increased. The L_n, L_w and coarseness decreased from 0.48 mm, 1.34 mm and 0.57 mg/m to 0.09 mm, 0.36 mm and 0.187 mg/m, respectively. However, the amount of fines increased up to 92.40%. In addition,

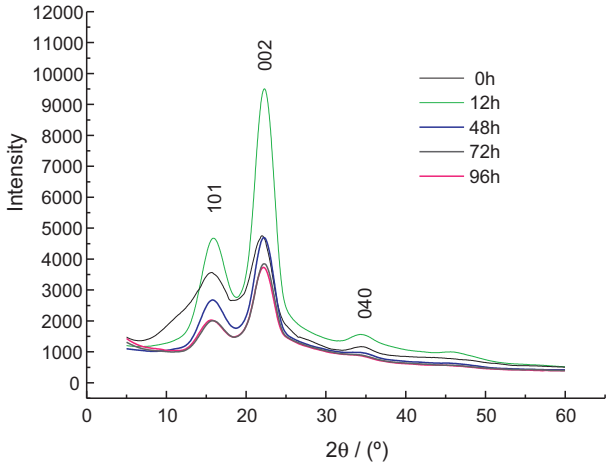

Fig. 4. The XRD patterns of bagasse solid base pulp after enzyme hydrolysis for different times.

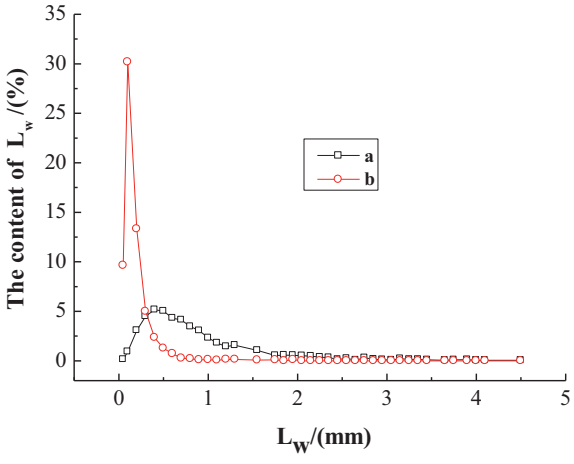

Fig. 5. The plot of length-weighted distribution of cellulose fibers (a stands for pulp, b stands for the pulp after enzyme hydrolysis for 72 h).

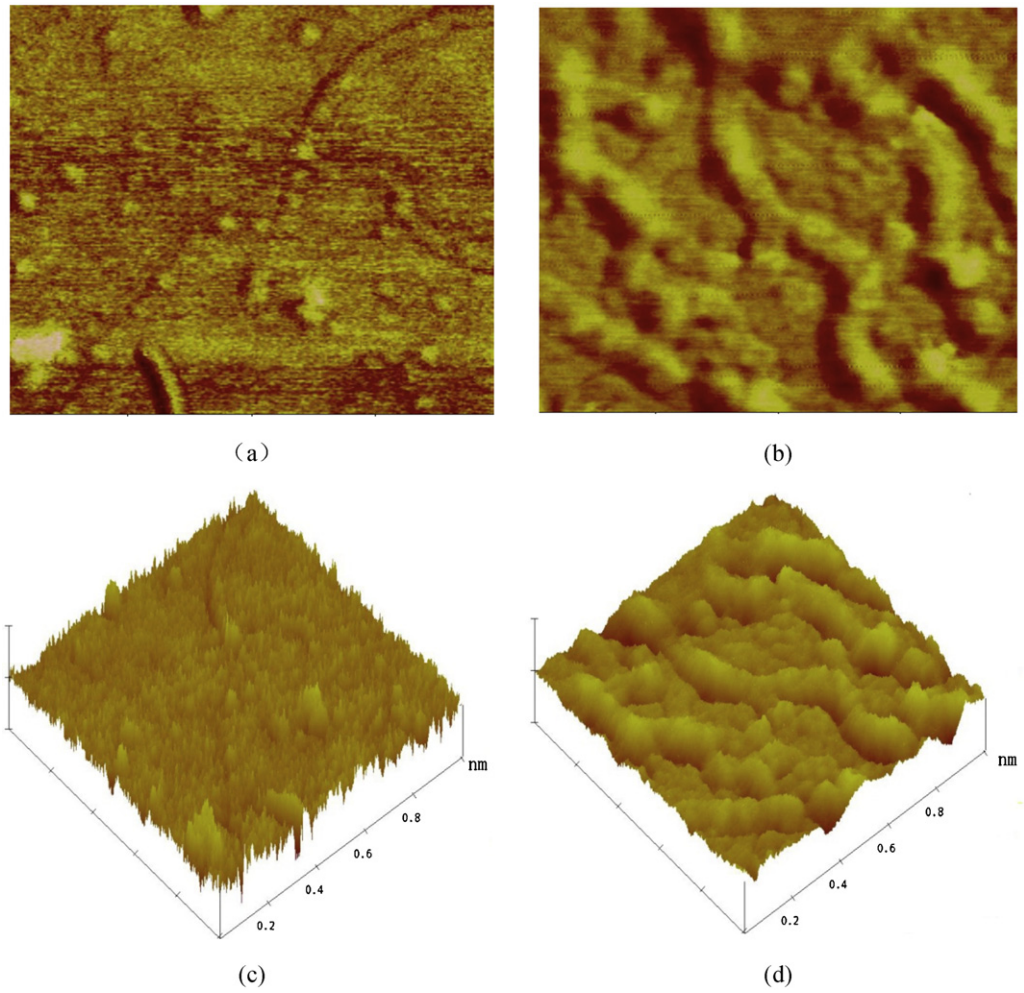

Fig. 6. The AFM phase images of pulp (a and c) and pulp after enzyme hydrolysis for 72 h (b and d) (dark–light = low–high; scan size: 1.0 nm × 1.0 nm; scan rate: 1.001 Hz).

the L_w/L_n also improved from 2.79 to 4.00. This finding showed that the fiber of bagasse pulp degraded greatly after enzymatic hydrolysis.

3.6. Atomic force microscopy (AFM)

The analysis of cellulose, lignin and extractive with AFM has been used for several years. Fig. 6 shows the AFM phase images of pulp (a and c) and pulp after enzyme hydrolysis for 72 h (b and d). It is believed that the nano-level test is focused at the single fiber surface. Thus, Fig. 6 shows the determination of the single fiber surface. As also can be seen from Fig. 6, the surface of bagasse pulp changes after enzymatic hydrolysis. The surface structure of the pulp before hydrolysis is observed to be highly granular (Fig. 6a and c) and is smoother than the pulp after hydrolysis (Fig. 6b and d). In addition, Fig. 6b and d indicates that the surface of pulp after hydrolysis gives more depressions. It is possible that the enzyme attacks the surface of cellulose resulting in release of some fragments of cellulose. However, the dark granules or blocks indicate that a material is more hydrophilic than the surrounding brighter granules or blocks (Gustalfsson, Ciovica, & Pltonen, 2003; Raghavan et al., 2000). Therefore, there are more blocks in Fig. 6d, meaning that the surface of pulp after hydrolysis is more hydrophilic than that of pulp before hydrolysis. From the above analysis, it is clear that the surface of cellulose of pulp is strongly disrupted by the cellulase and cellobiase treatment.

Table 2
The shape of cellulose fibers before and after hydrolysis.

Sample	L_n [a] (mm)	L_w [b] (mm)	(L_w/L_n)	Coarseness (mg/m)	Fines (%)
Before	0.84	1.34	2.79	0.570	24.39
After	0.09	0.36	4.00	0.187	92.40

[a] L_n stands for number-average-length.
[b] L_w stands for weight-average-length.

4. Conclusions

The present study described the enzymatic hydrolysis of bagasse pulp. Active oxygen pretreatment with solid base is considered as an environmentally friendly process due to no soluble base. Enzymatic hydrolysis of bagasse pulp revealed that when the amount of enzyme was 15 IU/g, the enzymolysis time was 72 h and the substrate concentration was 5%, the optimum sugar yield of 82.38% was obtained. However, the length of the cellulose fiber decreased and the crystallinity of cellulose had a cyclical variation after enzymatic hydrolysis. Furthermore, the surface of pulp after hydrolysis had more cavities or embossments and the surface characteristic of single fiber changed to be uneven and rough. Therefore, the treatment process with active oxygen and MgO-based solid alkali could accelerate the cellulose hydrolysis rate to fermentable sugars and the enzymatic hydrolysis of the bagasse pulp was more efficient.

Acknowledgments

The authors are grateful to the financial support from National Key Basic Research Program (2010CB732201) from the Ministry of Science and Technology of China, Natural Science Foundation of China (U0733001, 21106121), Basic Research Foundation for Central Universities from the Ministry of Education (2010121077) and Foundation of Scientific Research Universities (1270-K42004) from the Department of Economy and Commercial of Fujina Province of China.

References

Ardersen, K. H. (1998). *Deposit formation during coal–straw co-combustion in a utility PF-boiler*. Denmark: Technical University of Denmark.

Cao, Y., & Tan, H. (2005). Study on crystal structures of enzyme-hydrolyzed cellulosic materials by X-ray diffraction. *Enzyme and Microbial Technology*, *36*, 314–317.

Caputo, A. C., Palumbo, M., Pelagagge, P. M., & Scacchia, F. (2005). Economics of biomass energy utilization in combustion and gasification plants: Effects of logistic variables. *Biomass and Bioenergy*, *28*, 35–51.

Carrascoa, C., Baudela, H. M., Sendeliusa, J., Modig, T., Roslander, C., Galbe, M., et al. (2010). SO_2-catalyzed steam pretreatment and fermentation of enzymatically hydrolyzed sugarcane bagasse. *Enzyme and Microbial Technology*, *46*(2), 64–73.

Chunsheng, P., Tujun, X., Lu, L., Junping, Z., Ying, L., Jianbin, S., et al. (2012). Changes of the surface structure of corn stalk in the cooking process with active oxygen and MgO-based solid alkali as a pretreatment of its biomass conversion. *Bioresource Technology*, *103*(1), 432–439.

Elisabet, B., Marcus, Ö., & Anders, N. (2005). Mechanisms of bed agglomeration during fluidized-bed combustion of biomass fuels. *Energy & Fuels*, *19*(3), 825–832.

Gustalfsson, J., Ciovica, L., & Pltonen, J. (2003). The ultrastructure of spruce kraft pulps studied by atomic force microscopy (AFM) and X-ray photoelectron spectroscopy (XPS). *Polymer*, *44*, 661–670.

He, T., Rallming, Y., Weidong, S., & Shuangfei, W. (2010). Peroxide–acetic acid pretreatment to remove bagasse lignin prior to enzymatic hydrolysis. *Industrial and Engineering Chemistry Research*, *49*, 1473–1479.

Nelson, M. L., & O'connor, R. T. (1964). Relationship of certain infrared bands to cellulose crystallinity and crystal lattice type. II. A new infrared ratio for estimation of crystallinity in cellulose I and II. *Journal of Applied Polymer Science*, *8*(3), 1325–1341.

Raghavan, D., VanLandingham, M., Gu, X., & Nguyen, T. (2000). *Langmuir*, *16*, 9448–9459.

Rogers, J. G., & Brammer, J. G. (2009). Analysis of transport costs for energy crops for use in biomass pyrolysis plant networks. *Biomass and Bioenergy*, *33*, 1367–1375.

Schacht, C., Zetzl, C., & Brunner, G. (2008). From plant materials to ethanol by means of supercritical fluid technology. *Journal of Supercritical Fluids*, *46*, 299–321.

Stark, N. M., & Matuana, L. M. (2007). Characterization of weathered wood–plastic composite surfaces using PTIR spectroscopy, contact angle, and XPS. *Polymer Degradation Stability*, *92*(10), 1883–1890.

Sun, Y., & Cheng, J. (2002). Hydrolysis of lignocellulosic materials for ethanol production: A review. *Bioresource Technology*, *83*(1), 1–11.

Uihlein, A., Ehrenberger, S., & Schebek, L. (2008). Utilisation options of renewable resources: A life cycle assessment of selected products. *Journal of Cleaner Production*, *16*, 1306–1320.

Wei, G., Kim, D.-J., & Flemmin, G. (2003). Agglomeration in bio-fuel fired fluidized bed combustors. *Chemical Engineering Journal*, *96*(2), 171–185.

Xie, T.-J., Lin, L., Pang, C.-S., Yang, Q.-L., & Shi, J.-B. (2011). Effects of reactive oxygen on bagasse delignification and the cellulase hydrolysis. *Modern Food Science and Technology*, *27*(9), 1067–1073.

Yoshioka, T., Hirata, S., Matsumura, Y., & Sakanishi, K. (2005). Woody biomass resources and conversion in Japan: The current situation and projections to 2010 and 2050. *Biomass and Bioenergy*, *29*, 336–346.